

## Fabrication of nickel magnetic nanoparticles by combination of polyol and hydrothermal processes

N. N. Minh<sup>a,\*</sup>, H. T. N. Quyen<sup>b</sup>, T. T. Xuan<sup>a</sup>

<sup>a</sup>*Department of Materials Science, Heat and Surface Treatment, School of Materials Science and Engineering, Hanoi University of Science and Technology No.1, Dai Co Viet street, Hanoi, Vietnam*

<sup>b</sup>*Department of Foundry Materials and Technology, School of Materials Science and Engineering, Hanoi University of Science and Technology No.1, Dai Co Viet street, Hanoi, Vietnam*

Nickel magnetic nanoparticles have been successfully fabricated by combination of polyol process and hydrothermal treatment. In this research, the formation of Ni nanoparticles was determined by X-ray diffraction (XRD) and Ultraviolet–visible spectroscopy (UV-Vis). The morphology and size of nanoparticles were observed by using Transmission Electron Microscopy (TEM) while magnetic property of Ni nanoparticles have been characterized by vibrating sample magnetometer (VSM). The results indicate that the synthesized Ni nanoparticles are in spherical shape and the sizes of nanoparticles are in range from 3.1 nm to 5.7 nm depending on concentration of Ni<sup>2+</sup> ions. The magnetization study in nickel nanoparticles shows ferromagnetic interaction but close to superparamagnetic state and the magnetization decreases with the size reduction.

(Received January 24, 2022; Accepted May 9, 2022)

*Keywords:* Magnetic nanoparticles, Magnetic properties, Nanoparticles, Polyol process, Hydrothermal

### 1. Introduction

Magnetic nanoparticles are known as nanomaterials that consists of magnetic elements, such as iron, nickel, cobalt, chromium, manganese, gadolinium, and their chemical compounds [1, 2]. Their physical and chemical properties depend on the crystal structures, sizes, chemical components, and shapes of nanoparticles. Sometimes, these properties are also influence by the source of magnetic nanoparticles synthesized from technological process [3, 4]. Besides, the magnetic nanoparticles also possess some special magnetic properties such as superparamagnetism, high coercivity, low Curie temperature and high magnetic susceptibility [5, 6]. Nowadays, the magnetic nanoparticles are widely used in biomedicine, environmental science, mineralogy, informatics, as well as catalysis due to their attractive properties in physics and chemistry [7, 8].

For biomedical uses, biomedical applications of magnetic nanoparticles have shown promise in a number of applications, including treatment of diabetes and diabetic foot ulcers [9], magnetic hyperthermia, enhancing magnetic resonance imaging (MRI) data, supplementing tissue engineering efforts and improving the delivery of drugs to difficult to reach microniches [10-12]. In additions, magnetic nanoparticles can be also used in a wide variety of other applications such as magnetic inks [13], magnetic memory devices [14], and pathogen detection in foods [15].

For fabrication of magnetic nanoparticles, there are many methods to produce magnetic nanoparticles such as photolytic reduction, radiolytic reduction, solvent extraction reduction, microemulsion, polyol process and alcohol reduction have been developed for preparation of metal nanoparticles [16, 17]. In some recent reports, the polyol process started receiving a significant interest from researchers because of its advance in controlling particle size and preparing solvent. Several types of solvent which can use to produce fine nanoparticles are the

---

\* Corresponding author: minh.nguyennhoc@hust.edu.vn  
<https://doi.org/10.15251/DJNB.2022.172.597>

binary system of didodecyldimethylammonium bromide (DDAB)/toluene [18], the system of cetyltrimethylammonium bromide (CTAB), n-butanol, n-octane and water [19] or the solvent in the presence of hexadecylamine (HDA) and trioctylphosphine oxide (TOPO) [20] were reported. Although the polyol process has many advantages as mentioned above. However, this method often leads to the results that the synthesized nanoparticles have crystal structure, but their size is large, several tens of nanometers [21]. In order to synthesize nanoparticles with smaller sizes, several processes have been carried out, but they often result in the obtained nanoparticles with amorphous structure and low magnetism [22]. Therefore, in this study, we have synthesized nanoparticles by combining polyol and hydrothermal processes. The polyol process allows us to get small-sized nanoparticles while the hydrothermal process increases the crystal structure in the obtained nanoparticles. In this study, we used the system of polyvinyl alcohol (PVA) and ethylene glycol as solvent to produce magnetic nanoparticles.

## 2. Materials and methods

In this study, all the reagents used in the present study were obtained from HiMedia, India. The fabrication of nickel magnetic nanoparticles was carried out in ethylene glycol (as a solvent) and polyvinyl alcohol (PVA,  $M_w = 42,000$ ) (as a surfactant). In the reaction consideration, polyvinyl alcohol forms a stable layer to protect the Ni nanoparticles while sodium borohydride ( $\text{NaBH}_4$ ) was used as reducing agent to reduce  $\text{Ni}^{2+}$  ions from solution nickel chloride ( $\text{NiCl}_2 \cdot 6\text{H}_2\text{O}$ ). The fabrication of nickel magnetic nanoparticles was prepared as following:

Prepared solution of surfactant: a stock solution of polyvinyl alcohol (PVA,  $M_w = 42,000$ ) was prepared by dissolving with the ratio of 0.7g PVA in 5 ml  $\text{H}_2\text{O}$  at temperature surrounding  $80^\circ\text{C}$ . The stock solution was diluted with ethylene glycol to obtain the required concentration at 4,0%wt with using the magnetic stirrer.

Prepared solution of nickel ion salt: use 0.1M nickel salt solution was prepared by adding 1.19 g of Ni salt into 50 ml ethylene glycol in cone flasks. The solution gets green color after preparing. In this article, variation in total of nickel ions was also used to study the effect on the morphology, particle size, and nanoparticle size distribution of the Ni nanoparticles. The concentration of PVA and volume of reducing agent were fixed as in Table 1.

Table 1. Samples with different total mole of nickel ion.

No of samples	Used $V_{0.1M \text{ NiCl}_2}$ (ml)	$n_{(\text{Ni}^{2+})}$ (mol)	Used $V_{0.75M \text{ NaBH}_4}$ (ml)	Used concentration of PVA (wt%)
N-01	3.0	$3 \times 10^{-4}$	4.0	4.0
N-02	4.0	$4 \times 10^{-4}$	4.0	4.0
N-03	5.0	$5 \times 10^{-4}$	4.0	4.0
N-04	6.0	$6 \times 10^{-4}$	4.0	4.0
N-05	7.0	$7 \times 10^{-4}$	4.0	4.0

Prepared solution of reducing agent: use 1.425g of sodium borohydride was dissolved in 50 ml of ethanol for producing the solution with 0.75M. The stirrer was used to accelerate the dissolving rate for reducing  $\text{Ni}^{2+}$  ions in solution at room temperature.

Synthesis of Ni nanoparticles: firstly, 200 ml solution of surfactant was filled in an erlenmeyer flask at room temperature. Following step, the solution of nickel ion salt was added inside the erlenmeyer flask under stirring condition. To this solution, 4 ml solution of reducing agent also was added drop by drop slowly until it finished. The magnetic stirrer was still used for an additional 30 minutes before the synthesized solution was left in 6 hours for complete reactions. The final obtained solution is black with colloidal form. In this report, the solution of nickel ion salt was also used with different volumes as in Table 1 to study the effect of nickel ion concentration on the morphology, particle size, and nanoparticle size distribution of the Ni nanoparticles.

Precipitation of nanoparticles in colloidal condition: to get black cluster powders of Ni magnetic nanoparticles from colloidal solution, 2 ml of hydrazine (80%) was added into the black colloidal solution. After 2 hours at stirring constant, the black cluster powder was suspended at the bottom of beaker while the liquid portion became clearer. Centrifuge was used to separate the nanoparticle from the liquid portion. The powder was washed with ethanol several times. The Ni magnetic nanoparticles were stored in ethanol before doing hydrothermal treatment.

Hydrothermal treatment: it was known that Ni magnetic nanoparticles that synthesized by polyol process as resulting in amorphous form. Thus, synthesized nanoparticles were also used hydrothermal treatment to increase the crystal structure [23, 24]. In following step, the ethanol solution including Ni magnetic nanoparticles was transferred into a borosilicate glass vessel-lined autoclave with a stainless steel shell and it was hydrothermally treated at 200°C for 8 hours. Finally, the black powders of Ni magnetic nanoparticles were obtained by using centrifuge and washing with ethanol before they were dried in oven at 80°C for 6 hours.

Morphology of the synthesized nanoparticles was determined using transmission electron microscopy (TEM, Philips, Model: CM12). The X-ray diffraction (XRD) pattern of the synthesized nanoparticles powder was done with Cu K $\alpha$  radiation ( $\lambda=1.54021$  nm) on an X-ray diffractometer (XRD, Siemens, Model: D5000). The UV-Visible machine (UV/Vis, PerkinElmer, Model: LAMBDA 25) was also used to confirm formation of Ni magnetic nanoparticles. The absorbance spectra were determined in 10 mm optical path length quartz cuvettes with Perkin Elmer double beam spectrophotometer. The nanoparticles were taken out directly from the solution after doing hydrothermal treatment and it was dispersed in ethanol before UV-Visible test. The magnetic property of Ni magnetic nanoparticles was done with the vibrating sample magnetometer (VSM, MicroSense, Model: 10VSM). The weight of testing samples used in this study was 0.01 gram and the testing was carried out at room temperature (300 K). The magnetic properties were investigated with an applied field at  $-20$  kOe  $<H< 20$  kOe.

### 3. Results and discussion

Fig. 1(a) shows X-ray diffraction pattern of prepared nickel nanoparticles. The five characteristic peaks for nickel  $2\theta = 44.46^\circ$ ,  $51.72^\circ$ ,  $76.45^\circ$ ,  $92.93^\circ$  and  $97.83^\circ$ , corresponding to Miller indices (111), (200), (220), (311), and (222) respectively, were observed. The peaks were in agreement with the published data [25] and belonged to JCPDS 04-0850. These confirm that the nanoparticle powders showed the presence of pure face centered cubic (fcc) nickel peaks and there are no distinct diffraction peaks other than those from fcc-Ni is found in the sample. The XRD pattern also shows that there is no second phase of NiO present even though, they are easily to be formed as reported in some articles [26]. In addition, compound of Ni<sub>2</sub>B which often appears in the reaction between sodium borohydride and nickel salt was also not present. These indicate that there is no other impurity in synthesized product. Therefore, these results show that sodium borohydride can be used to reduce nickel ions in ethylene glycol to make high purity nickel nanoparticles [27]. In addition, the width of peaks of nickel nanoparticles is narrow. This also indicates that the synthesized nanoparticles are almost in crystal form after hydrothermal treatment.

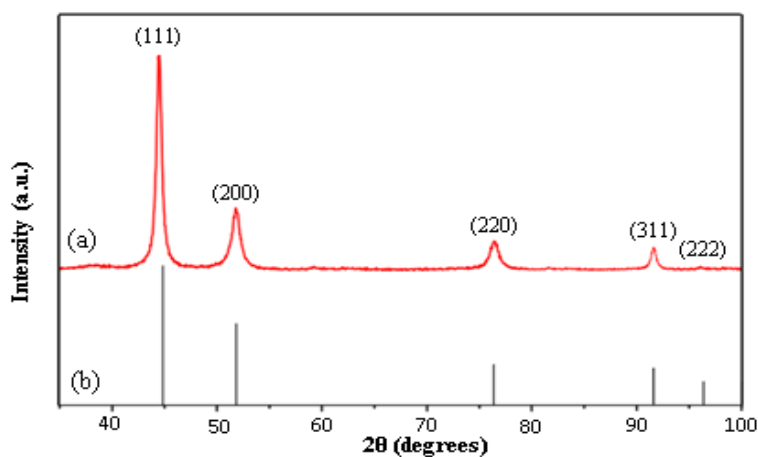
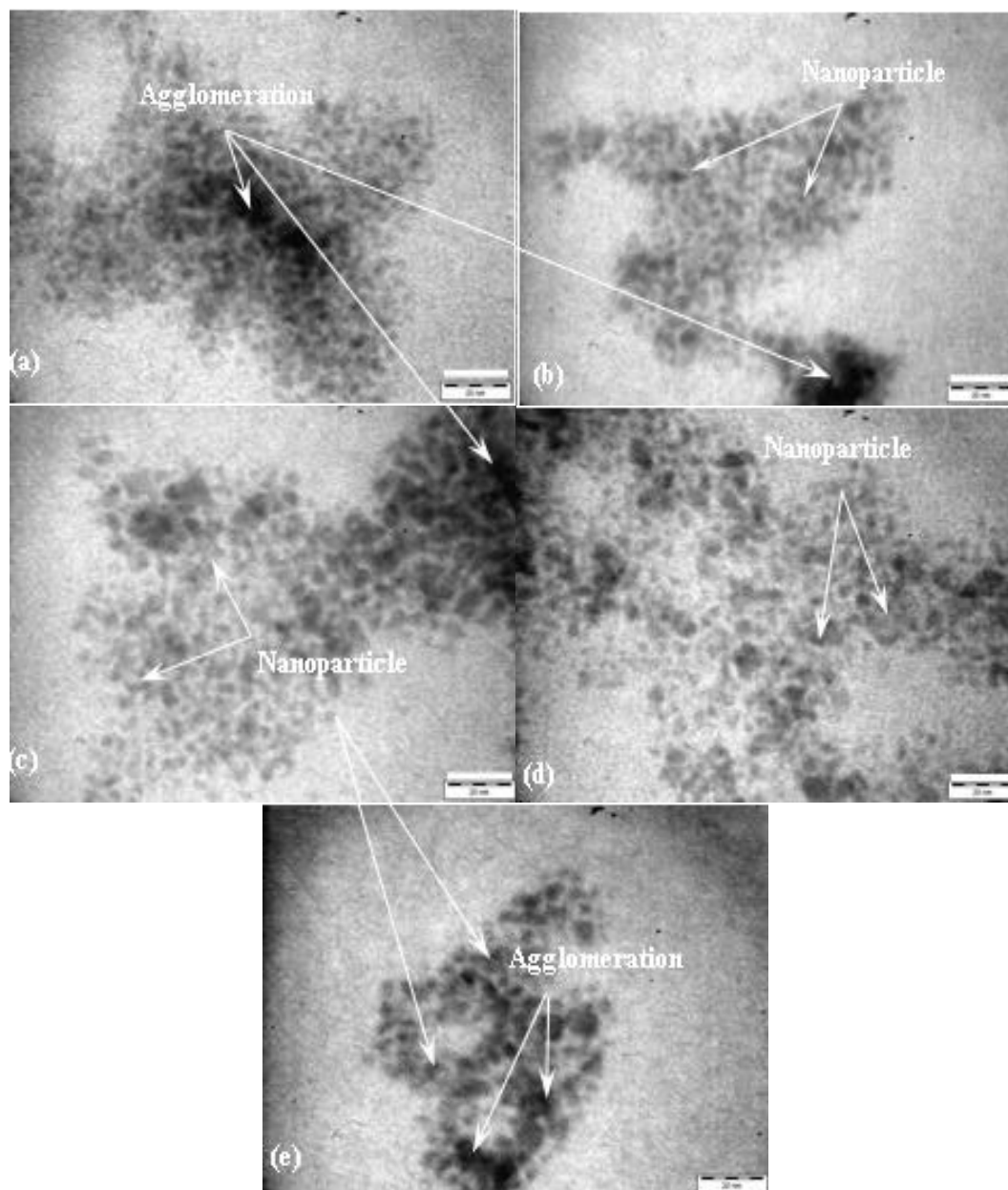


Fig. 1. XRD pattern of prepared nickel (a) and JCPDS file no. 04-850 (b).



*Fig. 2. TEM micrograph shows morphology of Ni magnetic nanoparticles at different concentration of nickel ions, sample N-01 (a); sample N-02 (b); sample N-03 (c); sample N-04 (d) and sample N-05 (e).*

To get TEM images, the black powder of Ni magnetic nanoparticles was dispersed in ethanol. The resulting solution was then taken out by using pipette and dripped onto a copper grid of TEM. The samples were dried under vacuum condition before observation. In Fig. 2, TEM micrographs confirm that morphologies of Ni magnetic nanoparticles at different concentration of nickel ions are all in spherical shape. TEM images at the same magnification also showed that difference between nanoparticle sizes in these images was not significant and this was observed on nanoparticle size distributions in Fig. 3.

Results in Figure 3 show the nanoparticle size distributions with various total mole of nickel ions. It can be seen that the particle size was proportional to total mole of nickel ions. With the increasing total mole of nickel ions, the particle size increased. Increasing the total mole of nickel ions will lead to higher frequency of particle collision thus resulting in a bigger particle size [28]. This can be observed in the particle size distributions, frequency of grains with larger mean

size was shifted on the right according to the increment of grains size: from position 4.0 nm with sample N-01 to position 4.3 nm of sample N-02 and with samples N-05 at position 4.7 nm. Besides, the increasing of total mole of nickel ions brought about increasing number of critical nucleation in solution and it leads to an acceleration of the growth of nanoparticles [29, 30]. This explained samples with high value of total mole of nickel ions would have frequent appearance of larger diameter grains such as 5.5 – 5.7 nm (sample N-05).

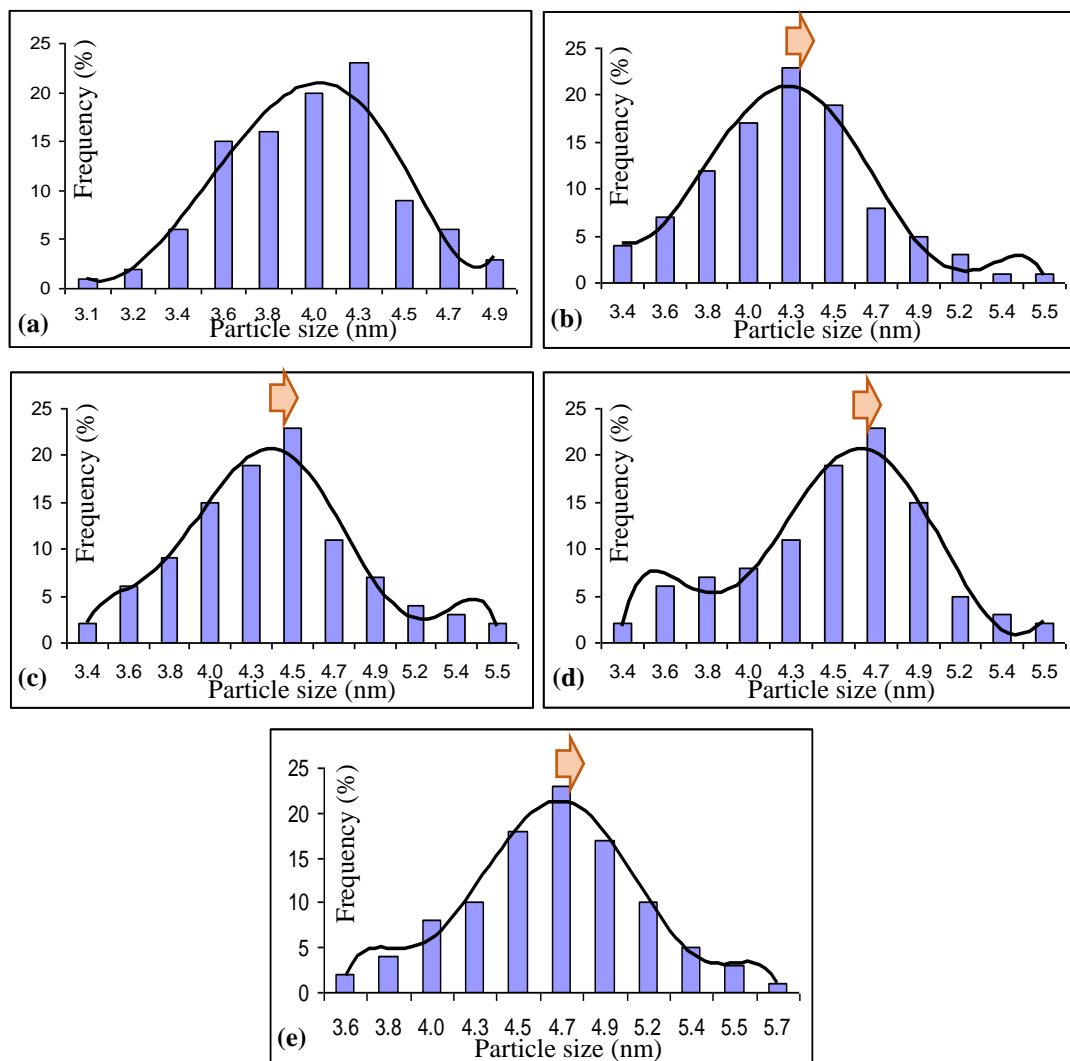


Fig. 3. Particle size distribution of samples with different concentration of nickel ions, sample N-01 (a); sample N-02 (b); sample N-03 (c); sample N-04 (d) and sample N-05 (e).

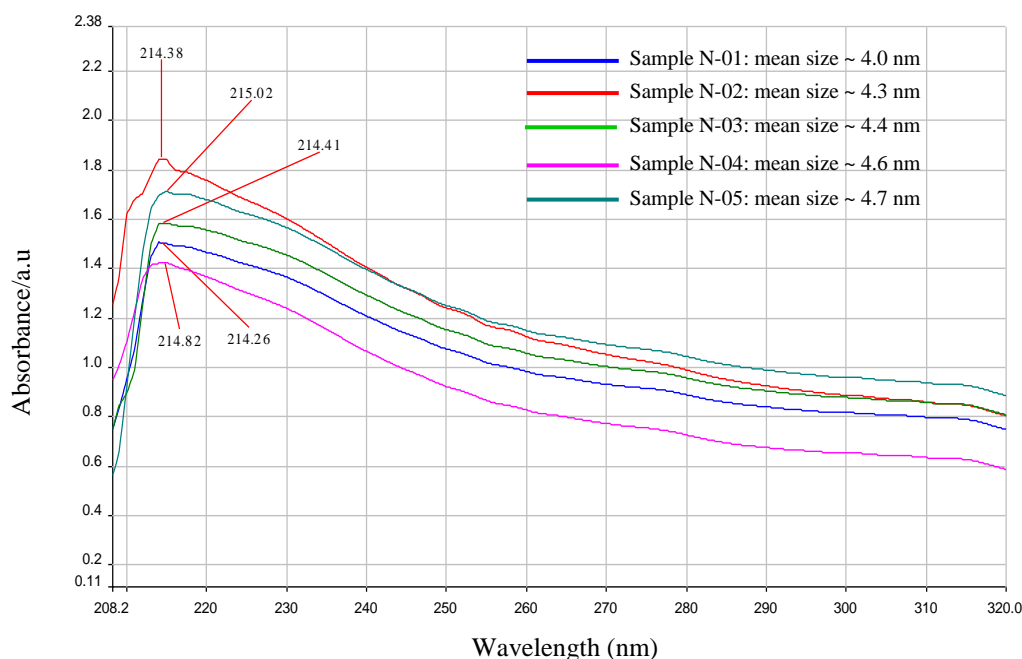


Fig. 4. Typical UV-visible spectra of samples with different total mole of nickel ion concentrations.

Fig. 4 shows the UV-Visible spectrum of samples with different total mole of nickel ions. It shows that the maximum absorption of wavelength increased when particle size increased. The absorption peak for sample N-01 with the smallest mean particle size 4.0 nm was at 214.26 nm and the intensity of plasmon band was 1.5. For the largest mean particle size, at value 4.7 nm of sample N-05, the maximum absorption of wavelength increased and reached at 215.02 nm with 1.71 for its intensity of plasmon band.

In our opinion, the optical absorption of metal nanoparticles has been described traditionally and classically by Mie theory as the localized surface plasmon resonance (LSPR) [31, 32]. These results based on Mie theory for the solid state which applies classical electrodynamics to simple shapes like spheres. So, we have assumed the resultant nanoparticles from ablation in ethanol to be spherical and widely spatially separated. The resulting Mie resonance cause selective optical extinction bands in the visible spectral range which usually depend strongly on the particle diameter [33]. For nanoparticle with larger mean size, the number of atoms required to make up the nanoparticles is enormous, so the number of conduction electrons is more than nanoparticles with smaller mean particle sizes. This results in increasing the maximum absorption of wavelength. However, difference between maximum absorptions of wavelength was not stated clearly here as the deviation between mean particle sizes of samples was too small as mentioned from the above TEM results. Besides, the UV-Vis results also showed that the only existing absorption spectrum region belongs to the Ni nanoparticles [34]. There are no absorption bands that belongs to other types of particles. This reinforces the conclusion from the above XRD result confirming that the synthesized nanoparticles are nickel nanoparticles.

Fig. 5 shows the hysteresis loops of nickel nanoparticle samples with different mean size. At room temperature, saturation magnetization ( $M_s$ ) of sample N-01, N-02, N-03, N-04 and sample N-05 are found to be 34.2, 37.5, 39.6, 41.3 and 42.4 emu/g, respectively. Results showed that reduction in magnetization is related to particle size effect. Decrease in  $M_s$  is due to reduce in particle size which can also results to increase in total surface area of testing sample. Due to small particle size surface to volume ratio increases and hence  $M_s$  reduces [35].

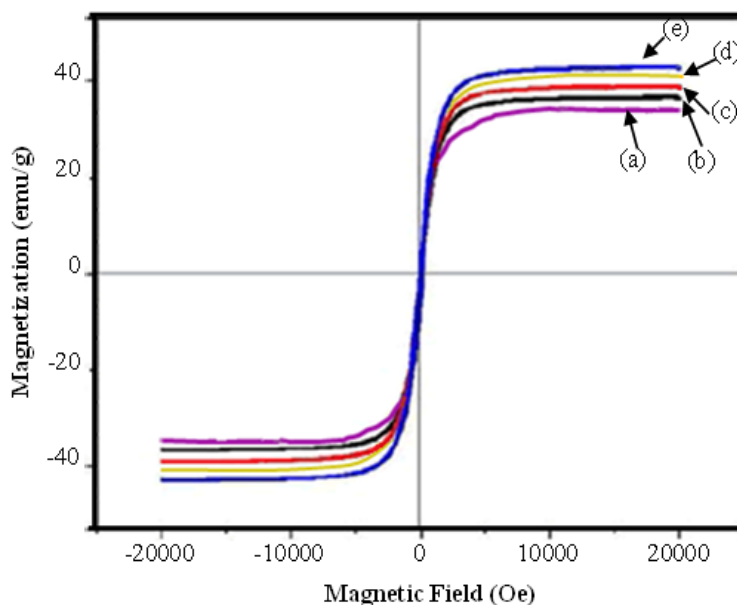


Fig. 5 The hysteresis loops of nickel nanoparticles, sample N-01 (a); sample N-02 (b); sample N-03 (c); sample N-04 (d) and sample N-05 (e).

However, the change in  $M_s$  value between samples is not much because the difference in mean particle size is not significant as mentioned in the TEM results above. In Figure 5 also shows that the coercivity value of sample N-05 is smaller than sample N-01. It is because there are two main factors relate to coercivity ( $H_c$ ): particle size ( $D$ ) and shape anisotropy. It is well known that  $H_c$  of ferromagnetic nanoparticles with regular shape conforms to the rule of  $H_c \propto 1/D$ . Therefore, for the synthesized spherical samples, the sample N-05 with the larger nanoparticle size has the lower coercivity [36, 37]. In addition, the hysteresis loops can also be attributed to superparamagnetic behavior in synthesized nickel nanoparticles.

#### 4. Conclusions

The nickel magnetic nanoparticles can be fabricated by combination of polyol and hydrothermal processes. Polyvinyl alcohol (PVA) can be used as capping agent in synthesis of nickel magnetic nanoparticles, and it does not allow to form any metal boride due to chelation of boric acid by polyvinylalcol.

Magnetic property of nanoparticles depends on nanoparticle size, saturation magnetization ( $M_s$ ) reduces with decreasing in particle size. Magnetization study reveals that it closes to superparamagnetic state at room temperature.

#### References

- [1] M. Krajewski, M. Tokarczyk, T. Stefaniuk, H. Słominska, A. Malolepszy, G. Kowalski, S. Lewinska, A. Waniewska, *Materials Chemistry and Physics* 246, 122812 (2020); <https://doi.org/10.1016/j.matchemphys.2020.122812>
- [2] J. Kudr, Y. Haddad, L. Richtera, Z. Heger, M. Cernak, V. Adam, O. Zitka, *Nanomaterials* 7, 243 (2017); <https://doi.org/10.3390/nano7090243>
- [3] A. Paolo, *Nanomaterials* 11, 1297 (2021); <https://doi.org/10.3390/nano11051297>
- [4] V. A. Vicky, A. Ajay, W. Bevins, *European Journal of Nanomedicine* 5(1), 11 (2013).
- [5] A. Yadollahpour, S. Rashidi, *Oriental Journal of Chemistry* 31, 25 (2015);

<https://doi.org/10.13005/ojc/31.Special-Issue1.03>

[6] K. McNamara, S. M. Tofail, *Advances in Physics: X* 2(1), 54 (2017);

<https://doi.org/10.1080/23746149.2016.1254570>

[7] Y. Slimani, M. A. Almessiere, A. D. Korkmaz, S. Guner, H. Gungunes, M. Sertkol, A. Manikandan, A. Yildiz, S. Akhtar, S. E. Shirsath, A. Baykal, *Ultrasonics Sonochemistry* 59, 104757 (2019); <https://doi.org/10.1016/j.ultsonch.2019.104757>

[8] P. Thilagavathi, A. Manikandan, S. Sujatha, Jaganathan, K. Saravana, S. A. Antony, *Nanoscience and Nanotechnology Letters* 8(5), 438 (2016); <https://doi.org/10.1166/nnl.2016.2150>

[9] M. V. Vellayappan, S. K. Jaganathan, A. Manikandan, *RSC Advances* 6(115), 114859 (2016); <https://doi.org/10.1039/C6RA24590K>

[10] H. M. Williams, *Bioscience Horizons* 10, 1 (2017);

<https://doi.org/10.1093/biohorizons/hzx009>

[11] A. Wu, P. Ou, L. Zeng, *NANO: Brief Reports and Reviews* 5, 245 (2010);

<https://doi.org/10.1142/S1793292010002165>

[12] E. C. Abenojar, S. Wickramasinghe, J. Bas-Concepcion, A. C. S. Samia, *Progress in Natural Science: Materials International* 26(5), 440 (2016); <https://doi.org/10.1016/j.pnsc.2016.09.004>

[13] P. Tiberto, G. Barrera, F. Celegato, M. Coisson, A. Chiolerio, P. Martino, P. Pandolfi, P. Allia, *The European Physical Journal B* 86, 173 (2013);

<https://doi.org/10.1140/epjb/e2013-30983-8>

[14] P. Malik, S. Pandya, V. Katyal, *International Journal of Advance Research* 1(1), 1 (2013);

<https://doi.org/10.1155/2013/327435>

[15] P. L. Ho, *Pathology* 46, S45 (2014); <https://doi.org/10.1097/PAT.000000000000060>

[16] F. Flievet, M. Souad, R. Brayner, F. Chau, M. Giraud, F. Mammeri, J. Peron, J. Y. Piquemal, L. Sicard, G. Viau, *Chemical Society Reviews* 47(14), 5187 (2018);

<https://doi.org/10.1039/C7CS00777A>

[17] S. H. Wu, D. H. Chen, *Journal of Colloid and Interface Science* 259(2), 282 (2003);

[https://doi.org/10.1016/S0021-9797\(02\)00135-2](https://doi.org/10.1016/S0021-9797(02)00135-2)

[18] J. P. Chen, C. M. Sorensen, K. J. Klabunde, G. C. Hadjipanayis, *Journal of Applied Physics* 76(10), 6316 (1994); <https://doi.org/10.1063/1.358280>

[19] E. E. Carpenter, A. Kumbhar, J. A. Weimann, H. Srikanth, J. Wiggins, W. Zhou, C. J. O'Connor, *Materials Science and Engineering: A* 286(1), 81 (2000);

[https://doi.org/10.1016/S0921-5093\(00\)00681-X](https://doi.org/10.1016/S0921-5093(00)00681-X)

[20] Y. Hou, H. Kondoh, T. Ohta, S. Gao, *Applied Surface Science* 241(1-2), 218 (2005);

<https://doi.org/10.1016/j.apsusc.2004.09.045>

[21] A. Parisien, F. A. Zarka, G. Hussack, E. A. Baranova, J. Thibault, C. Q. Lan, *Journal of Materials Research* 27, 2884 (2012); <https://doi.org/10.1557/jmr.2012.323>

[22] G. G. Couto, J. J. Klein, W. H. Schreiner, D. H. Mosca, A. J. A. Oliveira, A. J. G. Zarbin, *Journal of Colloid and Interface Science* 311(2), 461 (2007);

<https://doi.org/10.1016/j.jcis.2007.03.045>

[23] S. Asiri, M. Sertkol, S. Guner, H. Gungunes, K. M. Batoor, T. A. Saleh, H. Sozeri, M. A. Almessiere, A. Manikandan, A. Baykal, *Ceramics International* 44(5), 5751 (2018);

<https://doi.org/10.1016/j.ceramint.2017.12.233>

[24] R. A. Senthil, S. Osman, J. Pan, Y. Sun, T. R. Kumar, A. Manikandan, *Ceramics International* 45(15), 18683 (2019); <https://doi.org/10.1016/j.ceramint.2019.06.093>

[25] J. Tientong, S. Garcia, C. R. Thurber, T. D. Golden, *Journal of Nanotechnology* 2014, 1 (2014); <https://doi.org/10.1155/2014/193162>

[26] B. Chi, H. Lin, J. Li, N. Wang, J. Yang, *International Journal of Hydrogen Energy* 31(9), 1210 (2006); <https://doi.org/10.1016/j.ijhydene.2005.09.002>

[27] T. T. Co, T. K. A. Tran, T. H. L. Doan, T. D. Diep, *Journal of Chemistry* 2021, (2021).

[28] G. Nikki, F. G. Lauren, *Journal of Nanoparticle Research* 14, 760 (2012).

[29] C. Tojo, F. Barroso, M. D. Dios, *Journal of Colloid and Interface Science* 296(2), 591 (2006);

<https://doi.org/10.1016/j.jcis.2005.09.047>

[30] R. Andrea, Z. Marco, C. Massimiliano, M. Marco, P. Laura, A. Mauro, G. Rita, *Nanomaterials* 11(7), 1733 (2021).

[31] B. Gao, W. Duan, A. Silva, A. C. Walhof, W. Dai, F. Toor, *Optical Materials Express* 9(9), 3753 (2019); <https://doi.org/10.1364/OME.9.003753>

[32] G. Laila, S. Elias, G. Alham, H. S. Abdul, M. Khamirul, *Materials* 10(4), 402 (2017).

[33] S. Elias, G. Elham, N. Kazem, *International Journal of Molecular Science* 14(4), 7880 (2013).

[34] G. Elango, S. M. Roopan, K. I. Dhamodaran, K. Elumalai, N. A. A. Dhabhi, M. V. Arasu, *Journal of Photochemistry and Photobiology B: Biology* 162, 162 (2016);

<https://doi.org/10.1016/j.jphotobiol.2016.06.045>

[35] X. He, W. Zhong, C. T. Au, Y. Du, *Nanoscale Research Letters* 8, 446 (2013);

<https://doi.org/10.1186/1556-276X-8-446>

[36] J. S. Lee, J. M. Cha, H. Y. Yoon, J. K. Lee, Y. K. Kim, *Scientific Reports* 5, 12135 (2015).

[37] X. He, H. Shi, *Particuology* 10(4), 497 (2012); <https://doi.org/10.1016/j.partic.2011.11.011>